144 *Inorg. Chem.* **2010**, *49*, 144–149
DOI: 10.1021/ic901629k

Inorganic Chemistry
Article

Presence or Absence of a Central Se Atom in Silver Selenide/Selenolate Clusters with Halite Topology: Syntheses and Properties of $[(Ph_3PAg)_8Ag_6(\mu_6\text{-}Se)_{1-x/2}(SePh)_{12}]^{x+}$ (x = 0, 1)

Hari Pada Nayek, Werner Massa, and Stefanie Dehnen*

Fachbereich Chemie and Wissenschaftliches Zentrum für Materialwissenschaften, Philipps-Universität Marburg, Hans-Meerwein-Strasse, 35043 Marburg, Germany

Received August 14, 2009

Two types of Ph_3P/Ph ligated $Ag_{14}Se_{13-x}$ (x = 0, 0.5) clusters with halite topology were synthesized that differ by the occupation/nonoccupation of the central position by a 13th Se atom and the resulting charge: neutral $[(Ph_3PAg)_8Ag_6(\mu_6\text{-}Se)(SePh)_{12}]\cdot 11THF$ (**1**) and ionic $[(Ph_3PAg)_8Ag_6(\mu_6\text{-}Se)_{0.5}(SePh)_{12}][R_3SnCl_2]\cdot n$THF (R = Ph, n = 6 (**2a**); Cy, n = 5 (**2b**)) are all based on a tetradecanuclear cluster. The structural response on the charge was rationalized by DFT calculations, and the optical absorption behavior was studied.

Introduction

Over the past decades, there has been considerable interest in the coordination chemistry of transition metal complexes containing organic thiolates, selenolates, or tellurolates due to their structural diversity[1−6] and potential application as precursors for materials,[7−10] antimicrobial drugs,[11] and models for the active site of metallothioneins.[12,13] The organic ligands protect the complexes from self-aggregation into the binary phases.

Due to the peculiarity of d^{10} metal chalcogenides, a huge variety of nanometer-sized chalcogenide clusters have been synthesized that are stabilized by means of organic or organoelement ligand shells. Among the multifaceted types of d^{10} metal chalcogenide clusters, there are many that combine organochalcogenolate and phosphine ligands at their surface to avoid the collapse of the clusters into the thermodynamically preferred binary chalcogenide. Examples are $[Zn_8Se(SePh)_{14}(PnPr_3)_2]$,[14a] $[Zn_{16}Te_{13}(TePh)_6(tmeda)_5]$ (tmeda = tetremethylethylenediamine),[14b] $[Hg_{32}Se_{14}(SePh)_{36}]$,[15] $[Cd_{32}Se_{14}(SePh)_{36}(PPh_3)_4]$,[15] $[Cu_{144}Se_{73}(PPh_3)_{30}]$,[16] or the impressive record holder in metalchalcogenide cluster sizes, $[Ag_{490}S_{188}(StC_5H_{11})_{114}]$.[17] In most of the cases, the syntheses of the clusters start out from a metal complex—frequently formed from metal salts and phosphine ligands in situ—and a chalcogenide source that can also act as a chalcogenolate ligand.[14−17] Other ligands that serve to effectively inhibit the uncontrollable cluster growth into binary solids are diselenophosphates $[(RO)_2PSe_2]^-$ and allied ligands.[18] Some of the resulting compounds, like the octanuclear $[Cu_8(\mu_8\text{-}Se)\{Se_2P(OiPr)_2\}_6]_8$[19a] or $[Ag_8(\mu_8\text{-}Se)\{Se_2P(OiPr)_2\}_6]$,[19b] are

*To whom correspondence should be addressed. Tel.: 00496421-2825751. Fax: 00496421-2825653. E-mail: dehnen@chemie.uni-marburg.de.

(1) Dance, I. *Polyhedron* **1986**, *5*, 1037.
(2) Li, H.; Zhu, Y.; Cheng, M.; Ren, Z.; Lang, J.; Shen, Q. *Coord. Chem. Rev*. **2006**, *250*, 2059.
(3) Gerlach, C. P.; Christou, V.; Arnold, J. *Inorg. Chem*. **1996**, *35*, 2758.
(4) Liaw, W.; Lee, W.; Wang, C.; Lee, G.; Peng, S. *Inorg. Chem*. **1997**, *36*, 1253.
(5) Wang, X.-J.; Langetape, T.; Persau, C.; Kang, B. S.; Sheldrick, G. M.; Fenske, D. *Angew. Chem., Int. Engl. Ed*. **2002**, *41*, 3818.
(6) Tang, K.-L.; Xie, X.-J.; Zhang, Y.; Zhao, X.; Jin, X.-L. *Chem. Commun*. **2002**, 1024.
(7) Brennan, J. G.; Siegrist, T.; Stuczynski, S. M.; Steigerwald, M. L. *J. Am. Chem. Soc*. **1990**, *112*, 9240.
(8) Brennan, J. G.; Siegrist, T.; Stuczynski, S. M.; Steigerwald, M. L. *J. Am. Chem. Soc*. **1989**, *111*, 9233.
(9) Hector, A. L.; Levason, W.; Reid, G.; Reid, S. D.; Webster, M. *Chem. Mater*. **2008**, *20*, 5100.
(10) Jin, X.-L.; Xie, X.-J.; Qian, H.; Tang, K.-L.; Liu, C.-L.; Wang, X.; Gong, Q.-H. *Chem. Commun*. **2002**, 600.
(11) Nomiya, K.; Takahashi, S.; Noguchi, R. *J. Chem. Soc., Dalton Trans*. **2000**, 2091.
(12) Gasyna, Z.; Zelazowski, A. J.; Stillman, M. J. *J. Biol. Chem*. **1989**, *264*, 17091.
(13) Zelazowski, A. J.; Stillman, M. J. *Inorg. Chem*. **1992**, *31*, 3363.
(14) (a) Eichhöfer, A.; Fenske, D.; Pfistner, H.; Wunder, M. *Z. Anorg. Allg. Chem*. **1998**, *624*, 1909–1914. (b) Pfistner, H.; Fenske, D. *Z. Anorg. Allg. Chem*. **2001**, *627*, 575–582.
(15) Behrens, S.; Bettenhausen, M.; Deveson, A. C.; Eichhofer, A.; Fenske, D.; Lohde, A.; Woggon, U. *Angew. Chem., Int. Ed*. **1996**, *35*, 2215–2218.
(16) Krautscheid, H.; Fenske, D.; Baum, G.; Semmelmann, M. *Angew. Chem., Int. Ed. Engl*. **1993**, *32*, 1303–1305.
(17) Anson, C. E.; Eichhöfer, A.; Issac, I.; Fenske, D.; Fuhr, O.; Sevillano, P.; Persau, C.; Stalke, D.; Zhang, J. *Angew. Chem., Int. Ed*. **2008**, *47*, 1326.
(18) Lobana, T. S.; Wang, J.-C.; Liu, C. W. *Coord. Chem. Rev*. **2007**, *251*, 91–110.
(19) (a) Liu, C. W.; Hung, C.-M.; Santra, B. K.; Wang, J.-C.; Kao, H.-M.; Lin, Z. *Inorg. Chem*. **2003**, *42*, 8551. (b) Liu, C. W.; Shang, I.-J.; Wang, J.-C.; Keng, T.-C. *Chem. Comm*. **1999**, 995. (c) Liu, C. W.; Hung, C.-M.; Haia, H.-C.; Liaw, B.-J.; Liou, L.-S.; Tsai, Y.-F.; Wang, J.-C. *Chem. Comm*. **2003**, 976. (d) Liu, C. W.; Haia, H.-C.; Hung, C.-M.; Santra, B. K.; Liaw, B.-J.; Lin, Z.; Wang, J.-C. *Inorg. Chem*. **2004**, *43*, 4464.

 Published on Web 12/02/2009

Table 1. Details of the X-Ray Diffraction Studies[23]

compound	**1**·11THF	**2a**·6THF	**2b**·5THF
empirical formula	$C_{260}H_{268}O_{11}Ag_{14}Se_{13}P_8$	$C_{258}H_{243}Ag_{14}Se_{12.5}P_8O_6Cl_2Sn$	$C_{254}H_{253}Ag_{14}Se_{12.5}P_8O_5Cl_2Sn$
fw, g·mol^{-1}	6353.32	6374.05	6320.09
cryst syst	monoclinic	monoclinic	trigonal
space group	$P2_1/c$	$I2/a$	$R\bar{3}$
a, Å	31.7987(9)	24.7467(19)	20.3517(4)
B, Å	22.9837(4)	26.8921(15)	20.3517(4)
C, Å	33.2185(8)	36.722(3)	99.087(3)
α, deg			
β, deg	92.257(2)	95.356(10)	
γ, deg			
V, Å^3	24259.0(10)	24332.0(3)	35542.5(15)
Z	4	4	6
ρ_{calcd}, g·cm^{-3}	1.724	1.740	1.772
$\mu(Mo_{K\alpha})$, mm^{-1}	3.163	3.199	3.283
abs. corr. $T_{min/max}$	0.631/0.880	0.630/0.819	0.627/0.821
2Θ range, deg	2−52	4−52	2−52
reflns measured	228133	114253	59101
independent reflns	47148	23438	15185
R(int)	0.18	0.0638	0.1371
ind. reflns ($I > 2\sigma(I)$)	15371	14478	6064
params	2724	1380	632
R_1 ($I > 2\sigma(I)$)	0.0743	0.0437	0.0956
wR_2 (all data)	0.1625	0.1067	0.2484
GoF (all data)	0.749	0.826	0.981
max. peak/hole, e$^-$·Å^{-3}	1.211/−1.419	2.967/−2.731	1.305/−1.228

known for their capability to encapsulate and also exchange main-group ions like E^{2-} (E = S, Se) or X^- (X = Cl, Br), leading to unusual bonding characteristics.[19]

Here, we present a neutral and two cationic silver selenide/selenolate complexes protected by selenophenolate groups that show a so far unprecedented tolerance for the occupation of the central position by a Se^{2-} anion, $[(Ph_3PAg)_8(SePh)_{12}(\mu_6\text{-}Se)Ag_6]$·11THF (**1**), $[(Ph_3PAg)_8(SePh)_{12}(\mu_6\text{-}Se)_{0.5}Ag_6][Ph_3SnCl_2]$·6THF (**2a**), and $[(Ph_3PAg)_8(SePh)_{12}(\mu_6\text{-}Se)_{0.5}Ag_6][Cy_3SnCl_2]$·5THF (**2b**). In addition to the experimental investigations, the structures and charges were rationalized by means of quantum chemical investigations using density functional theory (DFT)[20] methods.

Experimental Section

General. All synthesis steps were performed with a strong exclusion of air and external moisture (N_2 atmosphere at a high-vacuum, double-manifold Schlenk line or Ar atmosphere in a glovebox). THF and *n*-hexane were dried and freshly distilled prior to use. $(PPh_3)_3AgNO_3$[21a] and 1,4-bis(trichloro-stannyl)-butane[22] were prepared according to literature methods. Ph_3SnCl or Cy_3SnCl were used as received from Aldrich or ABCR chemicals.

Synthesis of $[(Ph_3PAg)_8Ag_6(\mu_6\text{-}Se)(SePh)_{12}]$·11THF (1). 1,4-Bis(trichlorostannyl)butane (0.098 mmol) and $[(Ph_3P)_3AgNO_3]$ (0.5916 mmol) were suspended in 10 mL of dry THF. The mixture was cooled to −40 °C, and $PhSeSiMe_3$ (0.6322 mmol) was added dropwise to it. It was then allowed to warm up to room temperature slowly. Crystals were obtained after one week upon layering 5 mL of the solution with 5 mL of *n*-hexane. Yield: 41%. Semiquantitative elemental analysis (EDX): $Ag_{1.06}Se_{1.0}P_{0.66}$ (calcd: $Ag_{1.08}Se_{1.0}P_{0.61}$).

Synthesis of $[(Ph_3PAg)_8Ag_6(\mu_6\text{-}Se)_{0.5}(SePh)_{12}][R_3SnCl_2]$·*n*THF (R = Ph, *n* = 6 (2a); R = Cy, *n* = 5 (2b)). $[(Ph_3P)_3AgNO_3]$ (0.2529 mmol) and Ph_3SnCl (**2a**) or Cy_3SnCl (**2b**) (0.2594 mmol) were suspended in 10 mL of dry THF. The solution was cooled to −40 °C, **R** = $PhSeSiMe_3$ (0.2529 mmol) was added dropwise. The mixture was allowed to warm up to room temperature slowly. Crystals were obtained after one week upon layering 5 mL of the solution with 5 mL of *n*-hexane. Yield: 48% (**2a**) and 35% (**2b**). Semiquantitative elemental analysis (EDX): $Ag_{14.02}Se_{12.73}P_{7.98}Sn_{1.0}Cl_{1.95}$ (calcd: $Ag_{14}Se_{12.5}P_8Sn_1Cl_2$) (**2a**), $Ag_{14.09}Se_{12.80}P_{8.63}Sn_{1.0}Cl_{1.80}$ (calcd: $Ag_{14}Se_{12.5}P_8Sn_1Cl_2$) (**2b**).

Spectroscopy. EDX analyses were performed using an EDX device, Voyager 4.0 from Noran Instruments, coupled with an electron microscope, CamScan CS 4DV. Data aquisition was performed with an acceleration voltage of 20 kV and 100 s of accumulation time. The following emitted radiation of the atoms was analyzed: Ag−L, Se−L, Sn−L, P−K, and Cl−K. UV−vis spectra were recorded on a Varian Cary 5000 UV/vis/NIR spectrometer in the range of 800−200 nm employing the double beam technique. The samples were prepared as suspensions in Nujol oil between two quartz plates. Photoluminescence spectra were measured in DCM solutions using a Varian Cary Eclipse photoluminescence spectrometer. Emission spectra were recorded upon excitation at 250 nm.

X-Ray Structure Determination. Data were collected on a diffractometer equipped with a Stoe imaging plate detector system IPDS2T using graphite-monochromized Mo Kα radiation (λ = 0.71073 Å) at 100 K. Structure solution and refinement were performed by direct methods and full-matrix least-squares on F^2, respectively, using SHELXTL software.[23] Final crystallographic data and values of R_1 and wR_2 are listed in Table 1. Relevant bond distances and angles are listed in Tables S1 and S2 (see Supporting Information). All compounds of this type − including related ones reported so far − suffer from strong disorder of some of the Ag and chalcogen atoms and THF molecules. Therefore, the refinement required an according split model. This way, even the very poor data set for

(20) (a) Parr, R. G.; Yang, W. *Density Functional Theory of Atoms and Molecules*; Oxford University Press: New York, 1988. (b) Ziegler, T. *Chem. Rev.* **1991**, *91*, 651.

(21) (a) Barron, P. F.; Dyason, J. C.; Healy, P. C. *J. Chem. Soc., Dalton Trans.* **1986**, 1965. (b) Miyoshi, N.; Ishu, H.; Kondo, K.; Murai, S.; Sonoda, N. *Synthesis* **1979**, 300.

(22) Jousseaume, B.; Riague, H.; Toupance, T. *Organometallics* **2002**, *21*, 4590–4594.

(23) Sheldrick, G. M. *Shelxtl 5.1*; Bruker AXS Inc.: Madison, WI, 1997.

(24) (a) Ahlrichs, R.; Bär, M.; Häser, M.; Horn, H.; Kölmel, C. *Chem. Phys. Lett.* **1989**, *162*, 165–169. (b) Treutler, O.; Ahlrichs, R. *J. Chem. Phys.* **1995**, *102*, 346–355.

compound **2b** could be used to determine its structure. Note that the structural parameters given in this paper may represent values between averaged atomic positions.

Methods of the Quantum Chemical Investigations. The density functional theoretical (DFT)[20] investigations were carried out by means of the program system TURBOMOLE[24] using the RIDFT program.[25] For the calculation of $\mathbf{1^c}$ (neutral cluster $[(H_3PAg)_8Ag_6(\mu_6\text{-Se})(SePh)_{12}]$), $\mathbf{2^{c1}}^+$ (oxidized cluster $[(H_3PAg)_8Ag_6(\mu_6\text{-Se})(SePh)_{12}]^+$ with unchanged elemental composition) and $\mathbf{2^{c2}}^+$ (charged cluster $[(H_3PAg)_8Ag_6(SePh)_{12}]^{2+}$ without central Se ligand), the Becke-Perdew BP86 potential[26a−c] was used together with def2-TZVP basis sets (TZVP = triple-ζ valence plus polarization);[26d] Ph groups of PPh_3 were replaced by H. An effective core potential (ECP-28)[26e] was employed for Ag atoms for both consideration of relativistic effects and reduction of the computational effort. The simultaneous optimizations of geometric and electronic structures were performed employing the C_1 ($\mathbf{1^c}$) or C_i symmetry ($\mathbf{2^{c1}}^+$, $\mathbf{2^{c2}}^+$), according to the crystallographic point group symmetries of the neutral (**1**) and charged cluster (**2**). Tables S1 and S2 provide experimental as well as calculated distances for **1** and **2** (see Supporting Information).

Results and Discussion

Syntheses. The title compounds were synthesized by the reaction of $(PPh_3)_3AgNO_3$[21a] with $PhSeSiMe_3$[21b] in the presence of 1,4-bis(trichlorostannyl)butane[22] (**1**), triphenyltin chloride (**2a**), or tricyclohexyltin chloride (**2b**) in THF as a powder or as greenish-yellow crystals from a THF/*n*-hexane mixture. Thus, the driving force of the generation of **1**, **2a**, and **2b** is the formation of stable NO_3SiMe_3. Different from our previous studies with Cu complexes,[27a] but similar to the reaction of a ditin organyl with $Pd(OAc)_2$,[27b] the role of the bis(trichlorostannyl)-butane for the synthesis of **1** is not obvious. However, the synthesis was (a) not possible without it, and (b) reactions with related monotin compounds led to different products (**2a** and **2b**) under the given conditions. We assume either catalytic activity or the suppression of a competitive reaction as the most probable explanations for the necessity of the presence of the compound. Although it has not been possible to clarify how exactly the 1,4-bis-(trichlorostannyl)butane takes part in such reactions, it is well-known that both Sn−Cl and Sn−C bond cleavage can occur, producing free, active valences at the Sn atom. The first is obvious from derivatization of such compounds into compounds like 1,4-bis(trichalcogenolatostannyl)butane.[27c] Sn−C bond cleavage is part of the precursor syntheses and can also be observed at the 1,4-bis(trichlorostannyl)butane under solvothermal conditions.[27a] A thorough study of the according processes is subject to future work. Complexes **1**, **2a**, and **2b** were characterized by means of single-crystal X-ray diffraction[23] and EDX analyses. According to these investigations, the neutral compound **1** is based on a $Ag_{14}Se_{13}$ cluster core, which differs from the average composition of the cationic cluster core in **2a** and **2b**, $Ag_{14}Se_{12.5}$. The charge of the cluster cations is compensated by triorganotin dichloride anions.

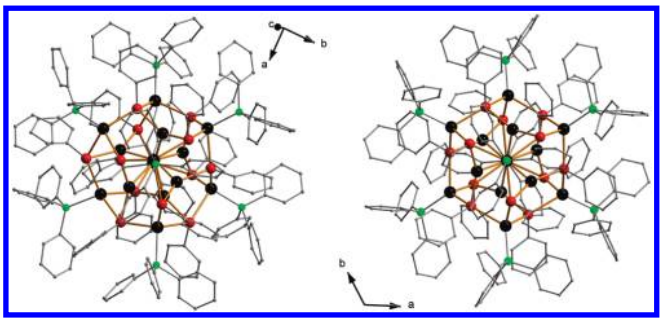

Figure 1. Molecular structures of the clusters in **1** (left-hand side) and **2b** (as a representative for **2a** and **2b**, right-hand side). Ag, black; Se, red; P, green; Sn, gray; Cl, blue; C, light gray. H atoms and disorder are not shown.

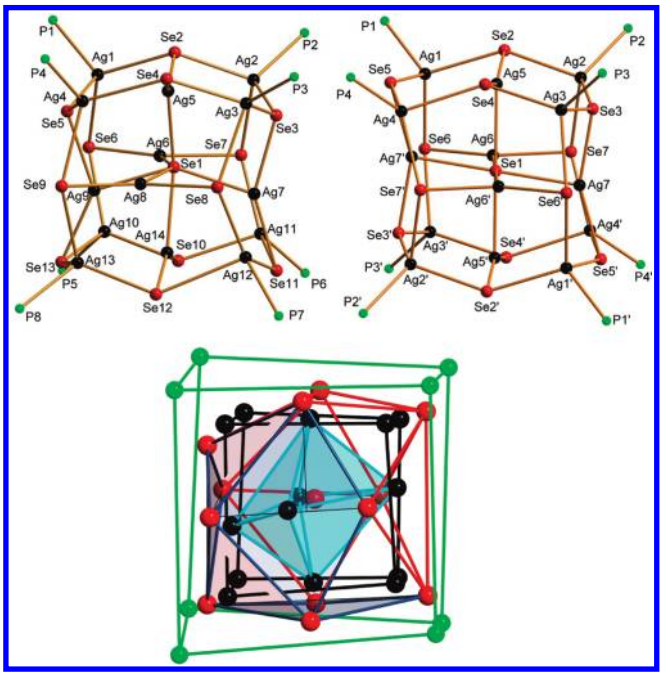

Figure 2. Cluster cores of compound **1** (left-hand side) and **2a** (as a representative for **2a** and **2b**, right-hand side) with the labeling scheme. Representation of the intertwining, nonbonding polyhedra in **1** as an example for all three clusters (bottom). Note that the central μ_6-Se atom is only present to 50% on average in **2a** and **2b**; that is, it is missing in every second cluster.

Crystal Structures. Compound **1** crystallizes in the monoclinic space group $P2_1/c$ with four formula units in the unit cell. Compounds **2a** and **2b** crystallize in the monoclinic space group $I2/a$ with four formula units in the unit cell and in the trigonal space group $R\bar{3}$ with six formula units in the unit cell, respectively. Figure 1 shows the molecular structures of **1** and **2b**, emphasizing the (pseudo)-D_{3d} symmetry, which is at least approximated by crystallographic C_3 symmetry in **2b**.

The $[Ag_{14}Se_{13-x}]$ cluster cores of compounds **1** (x = 0, Figure 2, left-hand side), **2a**, and **2b** (x = 0.5, Figure 2, right-hand side) can be described as highly distorted fragments of the halite topology.[28] The latter is encapsulated

(25) (a) Eichkorn, K.; Treutler, O.; Öhm, H.; Häser, M.; Ahlrichs, R. *Chem. Phys. Lett.* **1995**, *242*, 652–660. (b) Eichkorn, K.; Weigend, F.; Treutler, O.; Ahlrichs, R. *Theor. Chem. Acc.* **1997**, *97*, 119–124.

(26) (a) Becke, A. D. *Phys. Rev. A* **1988**, *38*, 3098–3109. (b) Vosko, S. H.; Wilk, L.; Nusair, M. *Can. J. Phys.* **1980**, *58*, 1200–1205. (c) Perdew, J. P. *Phys. Rev. B* **1986**, *33*, 8822–8837. (d) Weigend, F.; Ahlrichs, R. *Phys. Chem. Chem. Phys.* **2005**, *7*, 3297–3305. (e) Metz, B.; Stoll, H.; Dolg, M. *J. Chem. Phys.* **2000**, *113*, 2563.

(27) (a) Nayek, H. P.; Massa, W.; Dehnen, S. *Inorg. Chem.* **2008**, *47*, 9146–9148. (b) Nayek, H. P.; Niedermeyer, H.; Dehnen, S. *Dalton Trans.* **2009**, 4208–4212. (c) Nayek, H. P.; Niedermeyer, H.; Dehnen, S. *Z. Anorg. Allg. Chem.* **2008**, *634*, 2805–2810.

(28) Holleman, A. F.; Wiberg, E.; Wiberg, N. *Lehrbuch der Anorganischen Chemie*, 102nd ed.; Walter de Gruyter: Berlin, 2007; p 124.

Table 2. Ranges of Interatomic Distances in **1**, **2a**, and **2b**[a]

compound	**1**	**2a**	**2b**
$Ag_{oct}-\mu_6$-Se	264.3(2)−272.3(2)	281.08(5)−282.35(6)	279.3(3)−290.5(8)
$Ag_{oct}-\mu$-Se	254.1(2)−267.4(19)	251.4(2)− 255.47(10)	252.0(4)−254.9(4)
$Ag_{cube}-\mu$-Se	260.0(2)−306.6(2)	261.08(6)−285.18(8)	251.0(4)−292.0(4)
Ag−P	245.0(5)−256.1(5)	244.87(16)−251.11(15)	244.1(9)−249.3(8)

[a] Ag_{cube} and Ag_{oct} denote Ag positions at the eight vertices of the distorted cubic arrangement or the six faces, respectively.

by an organic shell of eight PPh_3 and 12 Ph groups. As in the halite topology itself, one might explain the cluster structures as consisting of four distorted polyhedra in an onion-type arrangement (Figure 2, bottom): around a central μ_6-Se atom, one observes a Ag_6 octahedron within a Ag_8 cube (i.e., the face-centered cube). The latter is intertwining with a Se_{12} polyhedron that represents a mixture ("centauer-polyhedron") of an icosahedron (red part in Figure 2) and a cuboctahedron (blue part in Figure 2). The whole is finally encapsulated by a P_8 cube. Table 2 summarizes ranges of the bond lengths in the clusters in **1** and the cluster cations in **2a** and **2b**.

The six Ag atoms of the Ag_6 octahedron bind to the μ_6-Se atom, and they bind to two further Se neighbors in a slightly distorted linear manner (μ-Se−Ag−μ-Se, **1**, 137.60(7)−148.18(7)°; **2a**, 147.1(3)−156.39(5)°; **2b**, 153.40(14)−161.18(8)°) to obtain a T-shaped coordination in the sum. The Ag atoms of the Ag_8 cube are located slightly above the centers of the eight triangular faces of the Se_{12} polyhedron and adopt a near tetrahedral coordination by one P and three Se atoms (Se−Ag−Se, **1**, 86.05(6)−127.54(13)°; **2a**, 94.19(3)−120.54(18)°; **2b**, 86.16(6)−124.9(8)°; P−Ag−Se, **1**, 95.40(10)−132.03(11)°; **2a**, 106.83(16)−121.59(17)°; **2b**, 102.77(12)−123.83(13)°). The selenolate Se atoms in turn act as μ_3 bridges to two Ag atoms of the Ag_8 cube and one Ag atom of the Ag_6 octahedron. The eight terminal PR_3 ligands point away from the vertices of the Ag_8 cube.

Disregarding the situation in the cluster center, the Ag/Se/P cluster cores of **1** and **2** are topologically identical to the homologous Ag/S/P cluster cores in $[Ag_{14}(\mu_6\text{-S})(SPh)_{12}(PPh_3)_8]\cdot 4CH_3OH\cdot 13H_2O$,[29a] the cation in $[Ag_{14}(\mu_6\text{-S})(Tab)_{12}(PPh_3)_8](PF_6)_{12}$ (Tab = 4-(trimethylammonio)benzenethiolate),[29b] the charge of which is, however, caused by zwitterionic ammonium-thiolate ligands, and the Ag/Te/P cluster core of $[Ag_{14}(\mu_6\text{-Te})(TePh)_{12}(PEt_2Ph)_8]$.[29c] However, in the cited compounds, the centers of the $[Ag_{14}S_{12}]$ face-centered cubes are always fully occupied, as in **1**, whereas a defect situation as observed in **2a** or **2b** was so far not reported.

The different bond lengths in **1** on the one hand and **2** on the other hand correspond to the different charge in both cluster types: in **2a** and **2b**, the $Ag_{oct}-\mu_6$-Se bonds are significantly elongated. This latter is in accordance with the observation that best refinement of the crystal structures with equally sized thermal ellipsoids was achieved for sof = 0.5 at the central μ_6 bridging Se position to account for the overall +1 charge. An obvious alternative model with a fully occupied Cl^- instead of the half-occupied Se^{2-} ion, the electron numbers of which are the same, cannot be ruled out by means of X-ray diffraction, though refinement of the Cl-containing model gives a little higher wR_2 and R_1 residuals for both structures **2a** and **2b**.[30] But in EDX analyses, 1.95 Cl atoms per Sn atom were found for **2a** and 1.80 for **2b**, instead of 3.0 Cl atoms as expected for a Cl-centered cluster, which we consider a significant result.

Table 3. Ranges of Calculated Distances for $\mathbf{1}^{c}$, $\mathbf{2}^{c1+}$, $\mathbf{2}^{c2+}$ and the average of $\mathbf{1}^{c}$ and $\mathbf{2}^{c2+}$, Simulated with PH_3 Instead of PR_3 Groups Using DFT Methods

compound	$\mathbf{1}^{c}$	$\mathbf{2}^{c1+}$	$\mathbf{2}^{c2+}$	av ($\mathbf{1}^{c}$; $\mathbf{2}^{c2+}$)
$Ag_{oct}-\mu_6$-Se	269.9−273.3	280.6−282.1		
$Ag_{oct}-\mu$-Se	259.1−269.5	256.9−263.2	250.6−252.0	254.9−260.3
$Ag_{cube}-\mu$-Se	267.6−291.1	270.6−288.2	279.3−293.5	271.6−291.8
Ag−P	246.9−260.6	241.5−250.5	241.4−249.7	244.1−252.5

Thus, half of the clusters in **2** contain a central Se ligand, whereas the other half exhibit an empty cluster center. The structures of the statistically distributed neutral and +2 charged clusters in **2** are averaged over the crystal l, leading to somewhat elongated displacement parameters and, of course, to averaging of the interatomic distances (Tables 2 and 3). In addition, residual electron densities indicated the presence of a second slightly inclined cluster core orientation with small occupations refined in a split atom disorder model to 7.5(1) % for **2a** and 4.6(2) % for **2b**, respectively. The data set of compound **2b** is very poor, such that this compound is presented mainly as further indication for the existence of the charged species.

The charge of the clusters in **2a** and **2b** is compensated for by one $[R_3SnCl_2]^-$ anion per formula unit (R = Ph or Cy). In $[R_3SnCl_2]^-$, tin is bonded to three R groups and two chloride ligands, resulting in a distorted trigonal bipyramidal geometry. The anions additionally serve to connect the clusters by a Cl····H−C_{Ph} hydrogen-bonding interaction. In **2a**, these interactions align the clusters into one-dimensional chains running along the crystallographic [201] direction (Cl····H, 272.00(5) pm; Cl···H−Ph, 138.61(8)°; Figure 3), whereas in **2b**, one $[Cy_3SnCl_2]^-$ anion connects every six clusters by Cl···H−C_{Ph} hydrogen bonds from Cl1 or Cl2 to three adjacent clusters each around the crystallographic *c* axis (Cl···H, 277.3(3)−323.0(5) pm; Cl····H−Ph, 136.35(10)−158.38(2)°).

Quantum Chemical Investigations. DFT investigations[20] were performed for model compounds with PH_3 instead of PPh_3 groups, employing the program system TURBOMOLE,[24,25] in order to rationalize the unusual structural and charge features. A neutral cluster $[(H_3PAg)_8Ag_6(\mu_6\text{-Se})(SePh)_{12}]$ ($\mathbf{1}^{c}$) and two charged ones—with a

(29) (a) Jin, X.; Tang, K; Liu, W.; Zeng, H.; Zhao, H.; Ouynag, Y.; Tang, Y. *Polyhedron* **1996**, *15*, 1211. (b) Chen, J.; Xu, Q.; Zhang, Y.; Chen, Z.; Lang, J. *J. Orgmet. Chem.* **2004**, *689*, 1071. (c) Corrigan, J. F.; Fenske, D.; Power, W. P. *Angew. Chem., Int. Ed. Engl.* **1997**, *36*, 1176–1179.

(30) The poor solubility of complex **2a** in $CDCl_3$ and CD_2Cl_2 refrained us from obtaining good quality ^{77}Se NMR spectra.

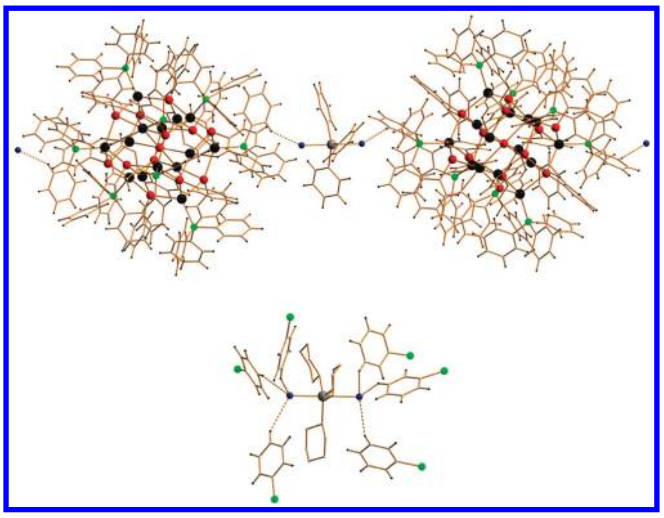

Figure 3. H···Cl hydrogen bonding in **2a** connecting two clusters within a one-dimensional chain along [201] (top) and a fragment of the H···Cl hydrogen bonding in **2b** along [001] (bottom), illustrating the linkage of six adjacent clusters that end up with a complicated three-dimensional network. Ag, black; Se, red; P, green; Sn, gray; Cl, blue; C, light gray; H, black small spheres.

central Se atom, $[(H_3PAg)_8Ag_6(\mu_6\text{-Se})(SePh)_{12}]^+$ ($\mathbf{2^{c1+}}$), or without a central Se ligand, $[(H_3PAg)_8Ag_6(SePh)_{12}]^{2+}$ ($\mathbf{2^{c2+}}$)—were calculated to exclude a pure oxidation of the cluster with unchanged composition ($\mathbf{2^{c1+}}$). The molecular structure of **1** is well-reproduced by the calculations (Table S1, Supporting Information, and Table 3), with maximum Δd = 15.5 pm at the longest $Ag_{cube}-\mu$-Se bond Ag12−Se12 (exptl: 3.066(2) pm) and smaller maximum deviations of Δd = 8.4 ($Ag_{oct}-\mu_6$-Se), 7.8 ($Ag_{oct}-\mu$-*Se*), and 8.1 pm (Ag−P) for the stronger bonds. For **2**, neither the structural parameters of the singly charged hypothetical species $\mathbf{2^{c1+}}$ nor those of $\mathbf{2^{c2+}}$ showed satisfying agreement with the observed structures (Table S2, Supporting Information, and Table 3). As expected, best agreement with the average bond lengths in **2** was achieved by averaging the structural parameters of $\mathbf{1^c}$ and $\mathbf{2^{c2+}}$ with maximum Δd = 11.6 pm at the $Ag_{cube}-\mu$-Se bonds, 6.0 pm for $Ag_{oct}-\mu$-Se and 5.2 pm at Ag−P bonds (vs **2a**).[31] The deviations observed for the singly charged species $\mathbf{2^{c1+}}$ are in a similar range but—untypical for DFT calculations—show in part significantly shorter bonds (up to −7.5 pm) than the experimental results. This, together with the fact that an oxidation of the cluster seems chemically questionable, gives strong evidence for the 1:1 mixture of an uncharged and a doubly charged cluster to be the most likely model. The calculations show identical trends on going from **1** to **2** (neutral to a charged one; 259.1−291.0 pm ($\mathbf{1^c}$) to 254.9−291.8 pm (av ($\mathbf{1^c}$; $\mathbf{2^{c2+}}$))) for the Ag−Se and (246.9−260.6 pm ($\mathbf{1^c}$) to 244.1−252.5 pm (av ($\mathbf{1^c}$; $\mathbf{2^{c2+}}$))) for Ag−P distances as observed in the experiment.

Optical Absorption and Emission Spectra. Single crystals of **1**, **2a**, and **2b** have been investigated by means of solid-state optical absorption spectroscopy. Solutions of the three compounds in dichloromethane were investigated by means of photoluminescence spectroscopy. Figure 4 shows the solid-state UV−vis spectra of the

(31) Note that owing to the poor quality of the crystal data for **2b** the compound was not considered for comparison with the calculations.

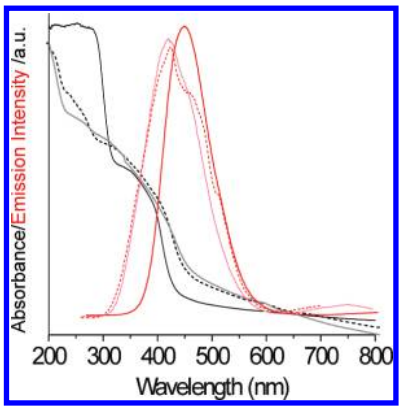

Figure 4. (Black) Solid-state UV−visible spectra of **1** (black solid line), **2a** (gray solid line), and **2b** (balck dashed line), recorded as suspensions of single crystals in nujol oil. Red: Photoluminescence spectra of **1** (red solid line), **2a** (pink solid line), and **2b** (red dashed line) in a dichloromethane solution.

compounds and the luminescence properties of **1**, **2a**, and **2b**.

Since both the silver and tin atoms possess a complete d^{10} shell according to the DFT study (formal Ag^I, Sn^{IV}), only Se(p) → M(s,p) charge transfer processes are expected for the absorption process. One observes an onset of absorption, that is, the lowest electronic excitation energy, at 433 nm (2.86 eV, **1**), 461 nm (2.68 eV, **2a**), and 458 nm (2.70 eV, **2b**), which are all in agreement with the observed color of the compounds. Further onsets of absorption are due to intraligand charge transfer processes involving the aromatic groups.

The emission spectra of the three compounds are dominated by the known luminescence of the PPh_3 ligand between 420 and 450 nm.[32] Therefore, the cluster heavy atoms are obviously not involved in the luminescence process; both emissions that are associated with Se^{2-} to Ag^+ charge transfer originating from triplet excited states as well as intrasilver d−s/d−p type transitions are expected to occur at distinctly lower energies.[33] As observed for the absorption properties, the emissions of the ionic compounds **2a** and **2b** are slightly different than those of the neutral cluster **1**. The emission λ_{max} of **2a** and **2b** (420 nm) is shifted by ca. 30 nm to higher energies with respect to **1**. Comprehensive theoretical studies are currently undertaken to gain further insight into the optical properties of the clusters, which are very demanding due to the large size of the complete clusters (420/421 atoms) and cannot be performed using the model compounds as they could for the structural investigations.

Several quantum chemical investigations—ab initio or molecular dynamics—and physical measurements were reported that served to study capture properties of silver clusters with fcc topology for small molecules like O_2 or CO.[34] All of these investigations took the tetradecanuclear fragment of the fcc packing as a model for the

(32) (a) Xie, Y.-M.; Wu, J.-H. *Chin. J. Struct. Chem.* **2007**, *26*, 1473–1475. (b) Wei, Y.-Q.; Wu, K.-C.; Zhuang, B.-T.; Zhou, Z.-F.; Zhang, M.-X.; Liu, C.-P. *Z. Anorg. Allg. Chem.* **2005**, *631*, 1532–1535. (c) Chandra, B. P.; Zink, J. I. *J. Phys. Chem.* **1982**, *86*, 4138–4141.

(33) Liu, C. W.; Shang, I.; Fu, R.; Liaw, B.; Wang, J.; Chang, I. *Inorg. Chem.* **2006**, *45*, 2335.

(34) See, for example: Avdeev, V. I.; Ruzankin, S. F.; Zhidomirow, G. M. *J. Struct. Chem.* **1997**, *38*, 519.

reactive Ag surfaces of silver metal. With our report on a potentially free site within a 14 silver atom Ag/Se cluster, we show that a similar host−guest situation—including small molecules or ions—might also be meaningful for silver chalcogenides.

Summary

Syntheses and characterization of three tetradecanuclear silver selenide clusters were reported, the Ag/Se cores of which are protected from further aggregation by Ph and PPh_3 groups. The clusters show similar, highly distorted halite-type topologies, however with two of the compounds revealing a partial loss of the central Se atom. The latter additionally provokes a positive charge of the defect cluster structures. DFT calculations helped to rationalize both the structural answer on the different compositions and very weak Ag−μ_6-Se contacts as an obvious precondition for the mobility of the central ligand. Ongoing work is dedicated to clarifying the so far unknown role of one of the precursors that seems to possess an indirect role in the cluster formation processes.

Acknowledgment. This work was financially supported by the German Science Foundation (DFG).

Supporting Information Available: Experimental and calculated bond lengths, EDX spectra, and X-ray crystallographic data for **1**, **2a**, and **2b** in CIF format. This material is available free of charge via the Internet at http://pubs.acs.org.